Journal of Radioanalytical and Nuclear Chemistry (2021) 328:347–358
https://doi.org/10.1007/s10967-021-07651-w

Efficient removal of U(VI) from aqueous solution using the biocomposite based on sugar beet pulp and pomelo peel

Mirza Nuhanović[1] · Narcisa Smječanin[1] · Nerma Curić[1] · Andrija Vinković[2]

Received: 8 December 2020 / Accepted: 18 February 2021 / Published online: 11 March 2021

Abstract

A biocomposite sorbent composed of sugar beet pulp and pomelo peel was utilized for the biosorption of uranium (VI) from the aqueous solution. Parameters such as solution pH, biocomposite amount, contact time, temperature and initial concentration of U(VI) ions on the adsorption performance of biocomposite sorbent was studied. The equilibrium data fitted best to the Langmuir's isotherm model ($q_{e,max} = 79.36$ mg g^{-1}). Obtained thermodynamic and kinetic parameters demonstrated that the biosorption process is spontaneous, exothermic, and fitted best to the pseudo-second order. The desorption study revealed that uranium recovery by 0.1 M $NaHCO_3$ was 99.24% in the first cycle for used biocomposite.

Keywords Uranium (VI) · Biocomposite · Equilibrium · Thermodynamics · Desorption

Introduction

Huge amounts of liquid radioactive waste are produced on a global level every day, and since the fissile isotope of uranium is the most used fuel in nuclear power plants, it appears as one of the main constituents of this type of waste. The presence of this radionuclide has a negative effect on all species and ecosystems due to its chemical and radiotoxicity, long half-life between 10^5 and 10^9 years and through the food chain, its toxicity to humans is unavoidable [1]. In natural waters, uranium is present in low concentrations, while in waters near mines and industrial plants, the concentration of uranium can reach significantly higher levels. The permissible discharge level of U(VI) in the wastewater of nuclear industries is in the range from 0.1 to 0.5 mg L^{-1} [2]. For this reason, uranium must be removed from such wastewater before discharging it into natural recipients.

Conventional methods for uranium removal from aqueous solutions include solvent extraction, chemical precipitation, reverse osmosis, ion exchange, ultrafiltration, and adsorption [3]. All the mentioned methods have proven to be effective in the treatment of uranium-contaminated wastewater. However, the limitations of these methods, such as high energy consumption, the creation of secondary pollution and incomplete removal, are unfavourable for the widespread popularization and promotion of these methods. Among these methods, adsorption, and within it biosorption, has an advantage over others due to its high efficiency and environmental friendliness [4, 5]. Biosorption is the process of removing pollutants of interest from aqueous solution using biological material and it enables the treatment of large amounts of effluents with a low concentration of sorbates of interest, low capital and operating cost, reduced amount of chemical or biological sludge, selective removal of metal ions, reduced use of toxic chemicals, rapid kinetics of adsorption and desorption, metal recovery and possibility of the biosorbent regeneration.

Previous studies have shown that biosorbents like algae, bacteria, fungi [6–8], and in recent researches different kinds of nanomaterials [9–11] and mesoporous materials [12–14] have good adsorption abilities for U(VI) removal from aqueous solution. However, in comparison to these, there are only a few studies regarding the biosorption of uranium by agricultural waste [15–18], and among these, all studies have concentrated on the uptake of uranium by agricultural biomass as individual and separate entities in native or modified forms. Biowaste from agricultural industries represents a low-cost adsorbent that possesses a lot of compounds such

✉ Mirza Nuhanović
mirzanuhanovic1.0@gmail.com

[1] Department of Chemistry, Faculty of Science, University of Sarajevo, Zmaja od bosne 33-35, 71000 Sarajevo, Bosnia and Herzegovina

[2] Ruđer Bošković Institute, Department of Experimental Physics, Bijenička cesta 54, 10000 Zagreb, Croatia

as pectin (galacturonic acid), hemicellulose, cellulose and lignin which have various polar functional groups, like carboxylic and phenolic acid groups that can be involved in metal ions complexion [19]. Additionally, the lignocellulosic material has shown very good chemical stability and mechanical strength due to its crystal structure. The biocomposite sorbents represent a composite material comprising of two or more materials that have a biological origin. Removal of uranium and similar radionuclides by adsorption onto biocomposite sorbents is insufficiently explored [20, 21] and there is a great potential in composite sorbents because biocomposites may display better characteristics of the effective biosorbents than its components individually.

This study regards removal of U(VI) from aqueous solution by biocomposite sorbent prepared as a combination of native forms of sugar beet pulp and pomelo peel and as a supporting material has been used silica gel. Key adsorption parameters were optimized and the nature of binding mechanism of U(VI)-biocomposite system was evaluated.

Materials and methods

Chemicals

All used chemicals were of analytical grade. Uranyl nitrate hexahydrate, Arsenazo III, 60% perchloric acid and silica gel (70–230 mesh) were purchased from Merck (Darmstadt), 85% phosphoric acid from Kemika and potassium hydroxide from Alkaloid (Skopje). The stock solution of U(VI) (1000 mg L^{-1}) was prepared by weighing 2.1308 g (Metler Tolledo balance, ± 0.1 mg) of $UO_2(NO_3)_2{\cdot}6H_2O$ salt analytical reagent grade. Working solutions were prepared by diluting the stock solution.

Batch experiments

Batch experiments were performed in a closed polypropylene bottle at 95–100 movements per min (mechanical shaker: Heidoplh Duomax 2030) to study the biosorption of U(VI) onto biocomposite sorbent. The experiments were performed by adding prepared biocomposite sorbent (50–500 mg) into a 50 mL solution containing a certain concentration of U(VI) (50–120 mg U/L). The filtrates were collected at suitable time intervals (0–120 min) at different temperatures (25, 35, 45 and 55 °C). The pH of each sample solution (3–9) was adjusted with 3.0 mol/L NaOH and measured by digital pH meter (CG 841 Schott-GERÄTE GmbH). All biosorption experiments were duplicated to make the results reliable and repeatable, and the mean values have been used for data evaluation because the variation of the experimental data was within the measurement error (±5%). The concentration of U(VI) ions in the filtrate, before and after sorption was determined spectrophotometrically at 650 nm by Arsenazo-III method on a UV–Vis spectrophotometer (model: Varian Cary 50) [22].

The removal efficiency (R, %) and sorption capacity of U(VI) ions (Q, mg L^{-1}) were calculated according to Eqs. (1) and (2).

$$R(\%) = \frac{C_i - C_f}{C_i} \cdot 100\% \quad (1)$$

$$Q = \frac{C_i - C_f}{m} \cdot V \quad (2)$$

where C_i and C_f are initial and final concentrations of U(VI) ions at the filtrate (mg L^{-1}), respectively, V is the volume of solution (L), and m is the mass of the biocomposite sorbent (g).

Biocomposite preparation

Sugar beet pulp was provided as a waste (fraction which remains after the production of sugar) from the Sunoko Sugar Factory (Novi Sad, Serbia). It was first washed by the tap water, then several times with smaller quantities of distilled water, air-dried for 24 h, and then dried in an oven at 80 °C ± 5 °C for 12 h. After cooling in a desiccator, sugar beet pulp was ground in a blender and powder was sieved through a standard sieve (∅ = 0.25 mm) and stored in a hermetically sealed container.

Pomelo was purchased at a local supermarket. Exocarp from the pomelo was removed from the fleshy mesocarp and cut into pieces of 0.5–1.0 cm, washed first by tap water, then several times with smaller quantities of distilled water, air-dried for 24 h, and dried in an oven at 80 °C ± 5 °C for 12 h. After cooling in the desiccator, the pomelo peel was ground in a blender, and the powder was sieved through a standard steel sieve (∅ = 0.25 mm). In this form, the powder of the native pomelo peel was stored in a hermetically sealed container.

For the preparation of the biocomposite, the procedure previously described by Akar et al. (2009) was used with some modifications [23]. 100 mL of 7% (w/v) aqueous solution of KOH was mixed with 10 g of silica gel and heated at 70–80 °C for 30 min. After cooling to 20 °C, the solution was mixed with a suspension containing 5 g of sugar beet pulp and pomelo peel. After a uniform mass was reached, 20% H_3PO_4 was added to the solution in a very small amount until a gel formulation was reached. The resulting gel was dried in an oven at 50 °C for 24 hours. After drying, the biocomposite was ground with mortar and pestle, sieved through a standard steel sieve (∅ = 0.25 mm) and stored in a hermetically sealed container for further sorption experiment.

Biocomposite characterization

To determine functional groups of prepared biocomposite from sugar beet pulp and pomelo peel, infrared spectra of the Fourier transform (FT-IR) were recorded on a Perkin Elmer BX FT-IR spectrometer using KBr pellet technique in a region from 4000 to 400 cm^{-1}. For the determination of the particle size distribution, the Malvern Mastersizer 2000 laser diffraction system with the wet dispersion unit Hydro 2000S (A) was used. This device is designed to determine the particle size distribution in the range of 0.2–2000 µm.

For the Energy Dispersive X-Ray Fluorescence (EDXRF) analysis, previously prepared biocomposite was additionally ground using mortar and pestle, sieved (∅ = 45 µm) and pressed into triplicate pellets weighing about 2 g with a diameter of 2.5 cm. Pellets were analysed using the EDXRF technique. The excitation source was a Siemens X-ray tube with Mo anode and Mo secondary target in orthogonal geometry. The tube operated at 45 kV and 35 mA and the irradiation time was 1000 s. Spectra were collected by a Canberra Si(Li) detector (3 mm thickness, 30 mm^2 active area, 0.025 mm Be window thickness) with a resolution of 170 eV (FWHM) at 5.9 keV. Samples were measured in vacuum. IAEA QXAS software was used for the analysis of spectra. Concentrations of K, Ca, Mn, Fe, Ni, Cu, Zn and Pb were determined by direct comparison of count rates using the IAEA-392 (Trace, minor and major elements in algae) standard reference material.

The value of pH_{pzc} (zero point of charge) is determined from the curve that intercepts the pH_i line of the plot ΔpH versus pH_i, where ΔpH represents a difference of pH_{final}-$pH_{initial}$ and pH_i is initial pH value of the buffered solution according to the previously described procedure by Zou and Zhao (2012) [24].

Desorption experiments

Desorption experiments were performed under optimal sorption parameters using the following desorption solutions: 1.0 M HNO_3, $NaHCO_3$ and citric acid to recover the adsorbed uranium from biocomposite. The percentage desorption from the spent biocomposite was calculated from the dose of U(VI) adsorbed onto biocomposite and the final U(VI) concentration in the desorption solution. To investigate the reusability of the biocomposite, consecutive adsorption-desorption cycles were repeated three times with the same biocomposite using previously determined desorption solution at different concentrations (0.25; 0.5; 1.0 M).

Results and discussion

Biocomposite characterization

FTIR analysis

The obtained FTIR spectrum of the prepared biocomposite is presented in Fig. 1. The wide peak at 3427 cm^{-1} is assigned to the stretching of O-H vibrations due to the stretching of the alcohols, phenols and carboxylic acids in pectin, cellulose and lignin which are the main constituents of the pomelo peel and sugar beet pulp. This peak may also indicate the presence of N-H stretching vibrations [25]. A peak at 2928 cm^{-1} corresponds to the stretching of C-H bonds in saturated aliphatic constituents [26]. The absorption band at 2378 cm^{-1} indicates the presence of a triple C≡C bond [21]. A peak at 1736 cm^{-1} is assigned to the stretching of the C=O bond in the ester groups [27]. The band at 1650 cm^{-1} can be attributed to the symmetrical stretching of the C=O bonds of carboxylates ($\nu_s(O_2C)$) and polyphenols (ν_s(O=C)). Additionally,

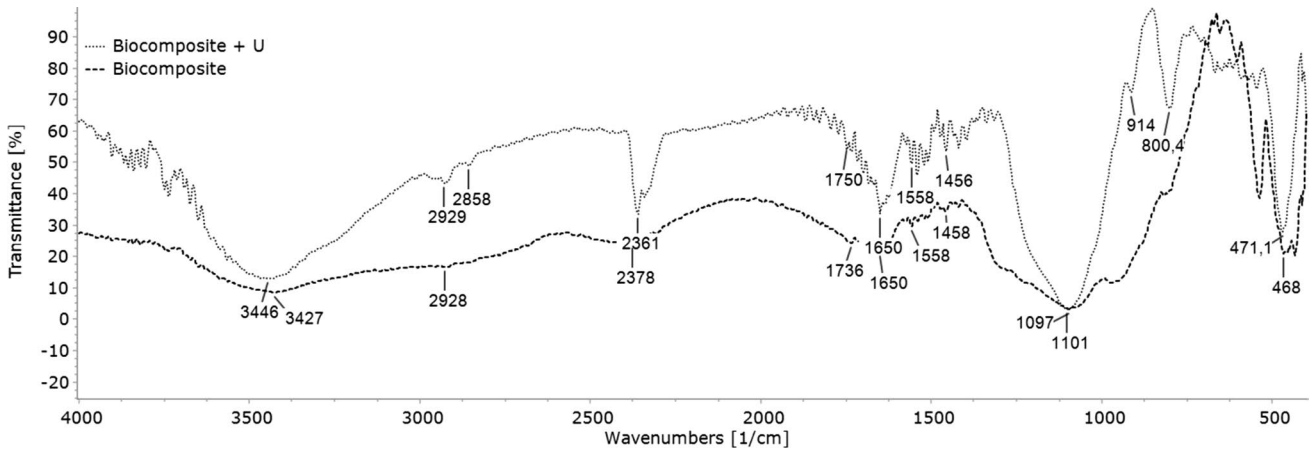

Fig. 1 FTIR spectra after and before sorption

the peak at 1650 cm^{-1} indicates a successful immobilization of the used components according to the study of Akar et al. [23] in which immobilization of *P. Vulgaris* was performed on activated silica gel. Symmetrical stretching of the C=C bonds of the aromatic systems of lignin and polyphenols can be attributed to a band of moderate intensity at 1558 cm^{-1}. A peak at 1458 cm^{-1} corresponds to the deformations of the C-H bonds of the various saturated cyclic rings, together with the deformations of the terminal methylene bonds (from -CH_2OH). This band predominantly originates from a symmetrical degenerate deformation of the methyl group of acetate and methoxy(poly)substituted aromatics, respectively. Since the immobilization of sugar beet pulp and pomelo peel was performed on activated silica gel, the band at 1097 cm^{-1} according to the literature indicates the presence of Si-O-Si bonds that are characteristic for silica gel. This peak was also found in the work of Akar et al. [23] and was taken as one of the indicators of successful immobilization.

The FTIR spectra of the loaded biocomposite showed which functional groups are involved in the sorption of uranyl ions (Fig. 1). The peak at 3427 cm^{-1} was shifted to 3446 cm^{-1} and the peak at 1736 cm^{-1} was shifted to 1750 cm^{-1}. Additionally, the change in band intensities in the region of 1600 to 1400 cm^{-1} could be observed. Furthermore, a new peak at 914 cm^{-1} is assigned to UO_2^{2+} stretching group which showed that sorption of uranyl ion was successful.

Zero point of charge (pH_{zpc}) of biocomposite

The pH_{pzc} of a biosorbent is a very important characteristic that determines the pH at which the biosorbent surface has net electrical neutrality. It is a characteristic of amphoteric surfaces and it is determined by the type of functional groups. Namely, the surface of the sorbent is positively charged in the case when the $pH < pH_{pzc}$ and shows an affinity for anions, while in the case when the surface is negatively charged, i.e. when the $pH > pH_{pzc}$, it shows an affinity for cations. The zero point of charge of the used biocomposite was 2.49 (Fig. 2), which is in accordance with the determined pH value (4). The obtained value indicates that below the pH value of the solution (2.49), the surface of the used biocomposite will be positively charged and will have a higher affinity for anions, while above this value surface of the biocomposite will be negatively charged and will have an affinity for positively charged cations, such as uranyl ions. Additionally, the obtained pH value is in accordance with the charge of the present functional groups on the surface of the used biocomposite.

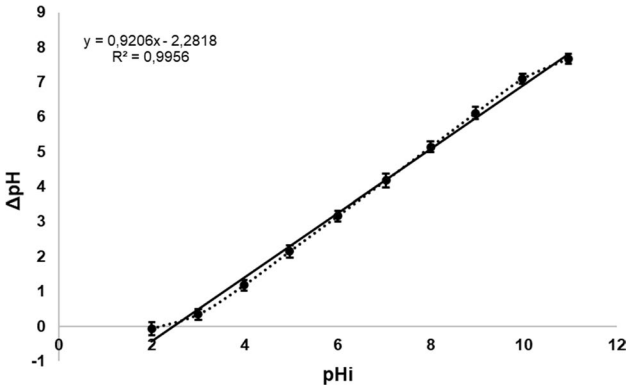

Fig. 2 The zero point of charge (pH_{pzc}) of biocomposite

Particle size distribution analysis (PSA)

According to the obtained results for the particle size distribution of the prepared biocomposite (Fig. 3) the highest percentage of the particles of large (˃ 90%) and medium diameter, and small particles are present in a small percentage. 10% of the particles are < 10.69 µm, 50% of the particles are < 113.96 µm and 90% of the particle are < 317.29 µm. Regarding the obtained results for the adsorption capacity of U(VI) onto used biocomposite, this particle size distribution resulted in a favourable biosorption process for U(VI).

EDXRF analysis

In modern times, the popularity of eco-friendly and low-cost biosorbents has increased. Thus the number of research on the applicability of agricultural waste has also increased, although the elemental concentrations of such waste when used as a biosorbent, are not investigated often. In the rice husk waste and its ash, researchers found that the main elements were C, O, Si and K, with smaller amounts of Ca, P, Mg and Cl [28, 29]. In the ground coffee waste and husks, the main elements were (in order of abundance) O, C, K, P, Mg, Ca and [29, 30]. The banana peel biosorbent had high concentrations of K and C and smaller concentrations of O, Ca, Si, P, S and Cl [31–33] while the mango peel analysed with EDX had only the C, O, K and Ca peaks visible [34, 35].

Biosorbent made of pomelo peel and sugar beet pulp as individual entities were also analysed by other researchers. Using the elemental analyser, Zhao and Chen (2020) found that the mass ratios of C, H and N in the unmodified pomelo peel were 40.55%, 6.134% and 1.441%, respectively [36]. Dinh et al. [37, 38] identified the only two visible peaks in the EDX spectra of the pomelo peel as O (52.59 wt%) and C (47.41 wt%). Sugar beet pulp biosorbent for uranium sorption was analysed by Nuhanović et al. [17] and it was found that the unmodified sugar beet consisted mostly of O and C,

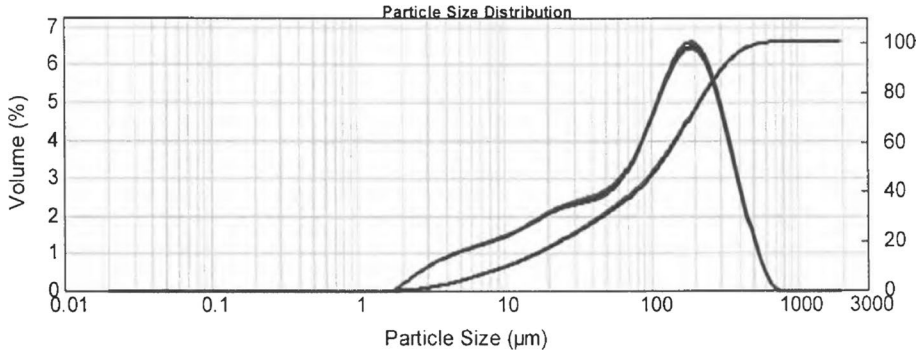

Fig. 3 The particle size distribution of the biocomposite

Table 1 Average values and standard deviations of the elemental concentrations measured in the pellets by EDXRF

Elemental concentrations	K (ppm)	Ca (ppm)	Mn (ppm)	Fe (ppm)	Ni (ppm)	Cu (ppm)	Zn (ppm)	Pb (ppm)
Biocomposite	70,060 ± 4762	3893 ± 394	7.1 ± 0.4	42.6 ± 2.6	0.65 ± 0.25	4.20 ± 0.56	6.94 ± 0.92	<MDL[a]

[a] <MDL - below the minimum detection limit (1.1 ppm for Pb)

with Si, Ca, Cu, S, Mg and K in smaller amounts and with the maximum adsorption capacity of 19.78 mg g^{-1} [17].

In the current research, composite biosorbent was made of pomelo peel, sugar beet pulp and silica gel. Concentrations of the eight elements measured in the triplicate pellets are presented in the form of an average value ± standard deviation and can be seen in Table 1. Using the EDXRF technique, it was found that the main elemental component of the used biocomposite was K, followed by Ca. In lesser amounts, Fe, Mn, Zn, Cu and Ni were also measured. Compared to the results of Nuhanović et al. [17], K is available in much higher concentration than Ca. Results obtained by EDXRF indicated that for uranium uptake by biocomposite except chemisorption involved mechanism could be also ion exchange.

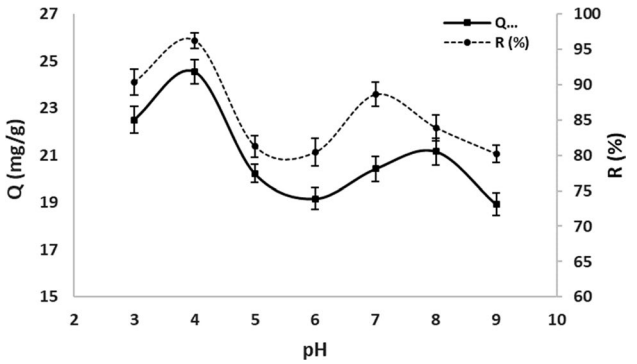

Fig. 4 Effect of pH on U(VI) adsorption capacity onto biocomposite (m = 100 mg; C_0 = 50 mg L^{-1}; V = 50 mL; T ≈ 25 °C; t = 60 min; shaking at 95–100 movements per min)

Effect of solution pH

The pH of the solution is a crucial parameter for the sorption studies of metal ions, as it affects the solubility and speciation of metal ions, surface charge and binding characteristics of the adsorbent [39]. From Fig. 4 it can be observed that the maximum adsorption capacity (24.55 mg g^{-1}) and removal efficiency (96.28%) for U(VI) was achieved at pH 4. The pH value of the zero point of charge for a biocomposite based on pomelo peel and sugar beet pulp was 2.49 and this value is lower than the experimentally determined optimal pH value at which the maximum adsorption capacity is reached, which means that the surface of the biosorbent will take a negative charge at determined optimal pH value. This further means that at a pH of the solution greater than pH_{pzc} (4 > 2.49) the change in surface polarity results in a favourable attractive electrostatic interaction between the negatively charged biosorbent surface and the positively charged uranyl species which was responsible for maximum adsorption performance at pH 4. Additionally, when the pH of the solution is low enough, divalent UO_2^{2+} is the dominant species of U(VI) in the solution. However, as the pH increases, the proportion of UO_2^{2+} in the solution decreases, while the proportion of monovalent hydrolysed species UO_2OH^+ and $(UO_2)_3(OH)_5^+$ increases, and monovalent metal species have an even greater affinity in ion exchange with protons because they can replace individual protons at separate binding sites on the biomass. Therefore, the increase in pH indicates good agreement for U(VI) adsorption due to the increase in the number of monovalent ions [40]. The decrease in the removal efficiency of U(VI) at higher pH values based on pH_{pzc} is because at pH > pH_{pzc} the surface of the biocomposite is negatively charged, which makes it, repulsive to anionic uranyl species such as

$UO_2(OH)_3^-$, $UO_2(OH)_4^{2-}$. Additionally, it could be due to the presence of insoluble inorganic carbon such as atmospheric CO_2 the formation of soluble ionic forms of uranyl carbonate ions, $UO_2(CO_3)_2^{2-}$ and/or $UO_2(CO_3)_3^{4-}$ as well as $(UO_2)_2(CO_3)(OH)_3^-$, which become the dominant stable anionic forms of uranium and to which the biosorbent used as a cationic ion exchanger don't have an affinity [41]. Also, at high pH, insoluble forms of uranium are formed (e.g. schoepite, $4UO_3 \cdot 9H_2O$) which reduce the overall efficiency of U(VI) biosorption at higher pH values [42]. Regarding all the above, pH 4 was selected as the optimal value and used in further testing.

Effect of biocomposite amount

As presented in Fig. 5 the adsorption capacity decreased with the increase of biocomposite amount. The maximum adsorption capacity (46.2 m mg g^{-1}) and removal efficiency (97.72%) was achieved with 50 mg of biocomposite dose. Decreased adsorption capacity of U(VI) ions can be due to partial aggregation and screening influence on the biocomposite surface which occurs at high biosorbent amount. Also, due to the increase of biocomposite amount mixing efficiency, the mass exchange could be slowed down [43]. Regarding the above, 50 mg was selected as the optimal mass of biocomposite for further biosorption experiments.

Adsorption kinetics

Kinetic modelling of the sorption process provides an insight into the velocity of the process and the mechanism of sorption, which includes mass transfer, diffusion and reaction on the surface of the biosorbent. The contact time influence onto uranium biosorption is presented in Fig. 6. Initially (0 to 15 min) the adsorption capacity increases to 44.8 mg g^{-1}. At the interval of 15–60 min these parameters value changes slowly, while after 60 min equilibrium

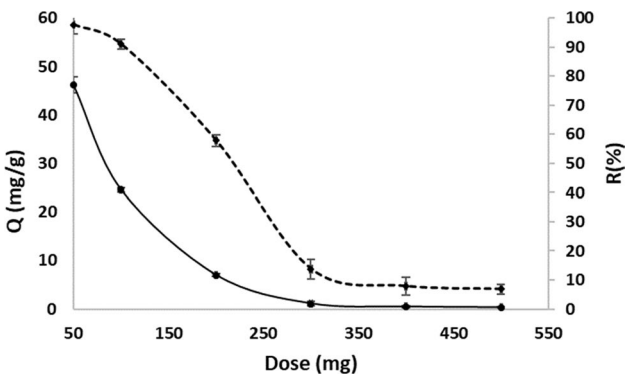

Fig. 5 Effect of biocomposite amount on U(VI) adsorption capacity onto biocomposite (C_0 = 50 mg L^{-1}; pH 4; V = 50 mL; T ≈ 25 °C; t = 60 min; shaking at 95–100 movements per min)

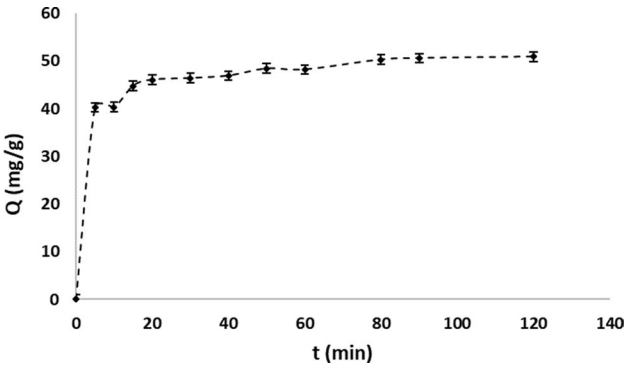

Fig. 6 Effect of contact time on U(VI) adsorption capacity (C_0 = 50 mg L^{-1}; m = 50 mg; V = 50 mL; T ≈ 25 °C; shaking at 95–100 movements per min)

is reached and maximum uranium sorption capacity of 48.2 mg g^{-1} was obtained. Finally, no significant changes in adsorption capacity were observed after 80 min. Based on the collected data, it can be concluded that the sorption process takes place through three stages. The first and fast stage (0–15 min) as a result of high free active sites concentration on the biosorbent surface and due to high initial metal concentration as a driving force. The second slower stage as a consequence of a free active centers number decrease and electrostatic repulsion which can also occur, by already bounded uranyl ions on the biocomposite [44]. At the last stage (80–120 min), a slight increase in the adsorption capacity (for only 2 mg g^{-1}) was the result of the mainly taken active sites on the biosorbents surface.

Applicability of the three commonly used kinetic models: Eq. (3) pseudo-first order model [45], Eq. (4) pseudo-second order model [46] and Eq. (5) intraparticle diffusion model [47] to the experimentally obtained results was investigated.

$$\ln(q_e - q_t) = \ln q_e - k_1 \cdot t \tag{3}$$

$$\frac{t}{q_t} = \frac{1}{k_2 q_c^2} + \frac{1}{q_e} \cdot t \tag{4}$$

$$q_t = k_{in} \cdot t^{\frac{1}{2}} + \tag{5}$$

where qe and q_t (mg g^{-1}) are the amounts adsorbed at equilibrium and at time t, respectively and k_1 (min^{-1}), k_2 (g $mg^{-1} \cdot min^{-1}$) and k_{in} (mg g^{-1} $min^{-1/2}$) are the rate constants of the pseudo-first order, pseudo-second order and the intraparticle diffusion kinetic model, respectively, while C (mg g^{-1}) is the constant of the model in the function of the boundary layer thickness.

Table 2 Kinetic parameters for uranium (VI) removal by biocomposite at 25.0 ± 0.5 °C and pH 4.0

Sorbent	$q_{e,exp}$	Pseudo-first order			Pseudo-second order			Intraparticle diffusion					
		$q_{e,cal}$	k_1	R^2	$q_{e,cal}$	k_2	R^2	k_{int1}	R_1^2	k_{int2}	R_2^2	k_{int3}	R_3^2
Biocomposite	51.9	12.3	0.033	0.946	51.5	0.00679	0.999	2.67	0.826	1.24	0.902	0.858	0.812

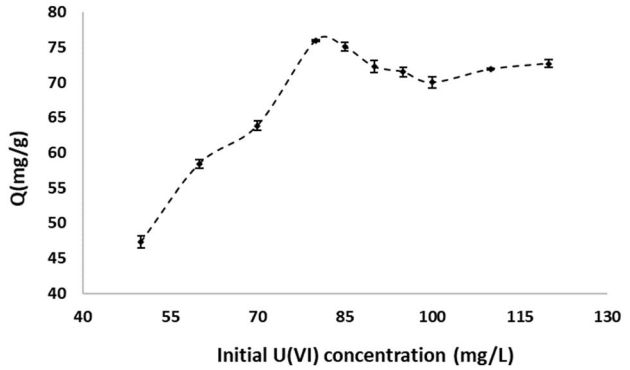

Fig. 7 Effect of initial U(VI) concentration on adsorption capacity (m = 50 mg; pH 4; V = 50 mL; t = 60 min; t ≈ 25 °C; shaking at 95–100 movements per min)

Linear correlation coefficient (R^2) values, as a measure of experimental data matching with the each proposed kinetic model, are shown in Table 2.

Pseudo-second-order model correlation coefficient (0.999) was higher in comparison to pseudo-first-order (0.946) and intraparticle diffusion kinetic models (0.826; 0.902; 0.812) with the closest calculated q_e value (51.5 mg g^{-1}) to the experimental (51.9 mg g^{-1}). The limiting step of the process (according to this model) is a chemisorption with a fast dynamic (equilibrium reached after 60 min). Additionally, the second intraparticle diffusion models phase also showed a good agreement with the obtained results describing sequential ion sorption, whereby the intraparticle diffusion of the ions into internal biosorbents channels and cavities limits the process velocity. Furthermore, ion exchange with more difficult replacing ions occurs, as well as the analyte binding to the active centers of biocomposite.

A complex mechanism of this U(VI)-biocomposite removal process could be defined as kinetically controlled by chemisorption combined with complexation and ionic exchange [48].

Adsorption isotherm

The initial U(VI) concentration in solution was varied in interval 50–120 mg L^{-1} at room temperature (25 ± 5 °C). According to the obtained results (Fig. 7), 80 mg L^{-1} was chosen as the optimal initial U(VI) concentration, with the maximum adsorption capacity of 75.99 mg g^{-1}.

Langmuir [49], Freundlich [50] and Temkin [51] adsorption isotherm models are expressed by linearized Eqs. (6, 8 and 9), respectively, fitting the experimental data:

$$\text{Langmuir: } \frac{1}{q_e} = \left(\frac{1}{K_L q_{max}}\right)\frac{1}{c_e} + \frac{1}{q_{max}} \tag{6}$$

Using Langmuir isotherm, a non-dimensional separating factor, R_L, describes the affinity between the analyte and biosorbent indicating the nature of the biosorption mechanism, which is given by the equation:

$$RL = \frac{1}{1 + K_L c_0} \tag{7}$$

The RL values in the range of $0 < RL < 1$ mark the biosorption process as favorable [49].

$$\text{Freundlich: } \log q_e = \log K_F + \frac{1}{n}\log c_e \tag{8}$$

$$\text{Temkin: } q_e = \left(\frac{RT}{b}\right)\ln(A_T) + \left(\frac{RT}{b}\right)\ln(c_e) \tag{9}$$

where equilibrated amount of analyte adsorbed per unit weight of sorbent material is q_e (mg g^{-1}), equilibrium concentration after adsorption is c_e (mg L^{-1}), maximum biosorption capacity is q_{max} (mg g^{-1}), Langmuir's isotherm constant associated with free energy of adsorption is K_L (L g^{-1}), Freundlich's constants indicating adsorption capacity are K_F (mg g^{-1}) (L $mg^{-1})^{1/n}$) and n (g L^{-1}), Temkin's equilibrium constant related to the maximum binding energy is A_T (L g^{-1}), the indicator of the heat of biosorption process is b (J mol^{-1}), the temperature is T (K) and a gas constant (8.314 J mol^{-1} K^{-1}) is R [51, 52]. The calculated adsorption isotherm parameters are presented in Table 2.

According to the obtained linear correlation coefficient values (Table 3), the sorption mechanism of U(VI) fits best to Langmuir model ($R^2 = 0.979$), regarding a sorption to a finite number of identical sites with a negligible interaction between adsorbed molecules. Therefore, U(VI) sorption onto biocomposite takes place on an energetically homogeneous surface (monolayer). The calculated maximum adsorption capacity, $q_{e,max} = 79.36$ mg g^{-1} matches to the experimental value, $q_{e,exp} = 75.99$ mg g^{-1}. Additionally, the sorption process of U(VI) onto used biocomposite is favorable due to separation coefficient value, $R_L = 0.0147$. Many similar studies reported that uranium sorption is

Table 3 Langmuir, Freundlich and Temkin isotherm parameters

Biosorbent	Langmuir				Freundlich			Temkin			$q_{e,exp}$
	$q_{e,max}$	K_L	R_L	R^2	K_F	1/n	R^2	RT/b	A_T	R^2	
Biocomposite	79.36	1.34	0.0147	0.979	53.06	8.38	0.814	320.65	9.34×10^{-4}	0.846	**75.99**

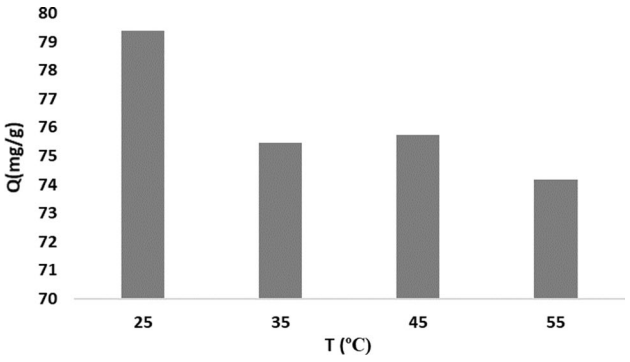

Fig. 8 Effect of temperature on uranium adsorption capacity onto biocomposite (C_0 = 80 mg L^{-1}, t = 60 min, pH 4, m = 50 mg, V = 50 mL, shaking at 95–100 movements per min)

better described by Langmuir's model than other models [17, 25, 53].

Adsorption thermodynamics

Temperature influence on U(VI) removal was investigated at four different values: 25, 35, 45 and 55 °C. The results shown in Fig. 8 indicate a temperature-independent U(VI) biosorption onto biocomposite with a maximum adsorption capacity of 79.38 mg g^{-1}. Regarding this, uranium adsorption capacity decreased as temperature raised. Therefore, the room temperature (25 °C) was chosen as an optimal and most suitable. As a not heat demanding process, the proposed removal system is very favorable in comparison to others [17, 54].

The following equations were used for a calculation of a thermodynamic parameters (shown in Table 4):

$$\Delta G = -RT\ln K_c \tag{10}$$

$$K_c = \frac{C_{Ac}}{C_e} \tag{11}$$

$$\log K_c = \frac{\backslash DeltaS}{2.303R} - \frac{\backslash DeltaH}{2.303R} \tag{12}$$

$$q_e = \left(\frac{RT}{b}\right)\ln(A_T) + \left(\frac{RT}{b}\right)\ln(c_e) \tag{13}$$

where change in the Gibbs free energy is ΔG (kJ mol^{-1}), temperature is T (K), gas constant ($8.314\cdot10^{-3}$ kJ mol^{-1} K^{-1}) is R, equilibrium constant is K_c, equilibrium concentration in the solution is C_e (mg L^{-1}) and the equilibrium concentration of the metal ion on the adsorbent is C_{Ac} (mg L^{-1}). Enthalpy change (ΔH, kJ mol^{-1}) and entropy change (ΔS, J mol^{-1} K^{-1}) values were obtained from the slope and intercept of Vant Hoff's plots of logKc versus 1/T [55].

Obtained thermodynamic data showed that the biosorption process of U(VI) by used biocomposite was spontaneous (high negative values of ΔG), exothermic (negative ΔH value − 38.637 kJ mol^{-1}), which also indicates that the energy released due to U(VI) binding onto sorbent is higher than the energy required for dehydration of metal ion [56]. Additionally, randomness increases as the reaction proceeds and the biosorption of U(VI) ions onto utilized biocomposite is a favorable process (suggested by positive ΔS value).

Desorption study

Desorption study is very important for the recovery of the adsorbed uranium and for the regeneration of the used biosorbent, which are important parameters for the practical application of the biosorption process. Additionally, the regeneration of the used biosorbents makes the process overally economically favorable. Three different desorption solutions were tested for the desorption study (Table 5).

$NaHCO_3$ showed the best results out of all tested eluents and was further investigated at three different concentrations (0.25; 0.5; 1.0). According to the obtained results, 1.0 M

Table 5 Removal efficiency after I cycle with different eluents

Eluents	1.0 M HNO_3	1.0 M $NaHCO_3$	1.0 M citric acid
Desorption efficiency (%)	44.18	95.98	43.35

Table 4 Thermodynamics parameters (ΔH, ΔS, ΔG)

Biosorbents	ΔH (kJ mol^{-1})	ΔS (J mol^{-1} K^{-1})	ΔG (kJ mol^{-1})			
			298 K	308 K	318 K	328 K
Biocomposite	− 38.637	0.1419	− 72.62	− 80.75	− 82.50	− 83.76

$NaHCO_3$ showed the highest desorption efficiency and it could be used for at least three cycles (Fig. 9). Obtained results in this study are opposite with the results for the biocomposite composed of *Ulva* sp. and Na bentonite [14], amidoximated *Saccharomyces cerevisiae* [57] and *Trichoderma harzianum* [58] for which the highest desorption efficiency was obtained with eluents, HNO_3 and HCl.

These results have shown that biocomposite based on pomelo peel and sugar beet pulp has a very good potential for the removal of U(VI) ions and its recovery.

Mechanism modelling

According to the results obtained from modelling data (biocomposite characterizations; adsorption kinetics; adsorption isotherms; adsorption thermodynamics) it could be observed that the mechanism of the U(VI) binding to the biocomposite is a complex and multi-step process [59]. FTIR spectra after sorption indicated that predominantly hydroxyl and amino groups are participating in the binding of uranyl ions, and a new peak at 914 cm^{-1} showed a presence of UO_2^{2+} onto biocomposite after sorption. EDXRF analysis showed that on the surface of biocomposite are present some of metal ions which can be exchanged with uranyl ions (Ca, K etc.) indicating possibility of ion exchange as one of the steps of the mechanism.

Furthermore, data showed that the process takes place through the three phases; equilibrium is reached very fast; the limiting step in the process is probably chemisorption and considering obtained data for intraparticle diffusion model, kinetic is not only controlled by one but by diverse processes. The process is temperature independent and occurs on the monolayer surface (Langmuir model). Even though according to pseudo-first order model the limiting step should be chemisorption, thermodynamic data are suggesting contrary. Thermodynamic data revealed that the process is spontaneous (negative ΔG values) and exothermic (negative ΔH value). However, physisorption occurs if the change in Gibbs free energy is in the range: − 20 to 0 kJ mol^{-1}, both physisorption and chemisorption occurs if values of ΔG are in the range: −20 to − 80 kJ mol^{-1} and chemisorption occurs if ΔG values are in the range: − 80 to 400 kJ mol^{-1}; so this data can indicate possible mechanism between sorbate and sorbent [60]. Calculated values of change in Gibbs free energy in the present study indicates both physisorption and chemisorption are occurring (Table 4). Furthermore, if $\Delta H > 0$ the main mechanism is a chemisorption, and if $\Delta H < 0$ the main mechanism is physisorption [61]. In the present study value obtained for ΔH (-38 kJ/mol) indicates exothermic nature of the process and physisorption. Considering that the capacity of adsorption (Fig. 8) decreased with an increase of temperature indicates also that physisorption occurred [62]. These results suggest both physisorption and chemisorption occurs on the surface of the used biocomposite at the same time and a layer of molecules may be adsorbed by physical forces on the top of an underlying layer with chemisorbed molecules [62–64].

With respect to all mentioned above, sorption of U(VI) onto biocomposite is a multi-phase process which is occurring with possible participation of both physiosorption/chemisorption, ion-exchange, and surface complexation.

Comparison of adsorption capacites

The comparison of adsorption capacity (q_{exp}, mg g^{-1}) of biocomposite used in this research with the adsorption capacities of various biosorbents and adsorbents reported in previous researches are given in Table 6 [17, 21, 39, 65–67]. According to the results obtained in this study, biocomposite could be considered as a potential sorbent for U(VI) removal from wastewaters, due to the adsorption capacity (75.99 mg g^{-1}) which is higher than many other sorbent materials. In addition, biocomposite is comprised of two types of agricultural wastes, pomelo peel and sugar beet pulp which are biodegradable, abundant, and low-cost material for which preparation is required minimum chemical consumption.

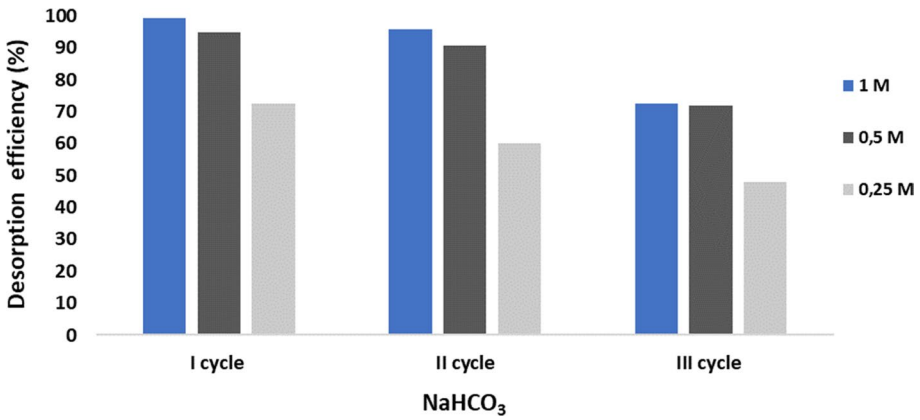

Fig. 9 Desorption efficiency after I, II and III cycles of desorption/adsorption with the three different concentrations of the eluent ($NaHCO_3$)

Table 6 Comparison of adsorption capacities of various sorbents for U(VI) removal

Sorbents material	Adsorption capacity (mg g^{-1})	References
Modified pomelo peel	270.71	[65]
Native sugar beet pulp	20.45	[17]
ACSD composite adsorbent (alginate, sepiolite, $CaSO_4 \times H_2O$ and diatomite)	3.51	[66]
Ceratophyllum demersum	140.45	[39]
Chitosan-modified zeolite	16.4	[67]
Bi-functionalized biocomposite adsorbent	43.2	[21]
Biocomposite (pomelo peel and sugar beet pulp)	75.99	Present study

Conclusions

In this study, a biocomposite sorbent composed of sugar beet pulp and pomelo peel was employed for the biosorption of U(VI) from aqueous solution. According to the obtained results prepared biocomposite can be used as a sorbent for the removal of U(VI) from the aqueous solution under the optimum conditions of pH 4, biocomposite dosage 50 mg, initial uranium concentration 80 mg L^{-1}, contact time 60 min, temperature 298 K with the maximum adsorption capacity of 75.99 mg g^{-1}. The equilibrium data fitted best to the Langmuir isotherm model and pseudo-second order. The results of the thermodynamic analysis indicated that the biosorption process of U(VI) uptake was exothermic and spontaneous. The biocomposite characterization confirmed its removal efficiency due to the numerous functional groups, particle size distribution and pH_{pzc} value that is in accordance with the pH of the solution (negatively charged surface of biocomposite). Additionally, the adsorbed U(VI) desorbed quantitatively by 1.0 M $NaHCO_3$ and biosorbent can be reused for three and more cycles. Regarding all the above, the involved mechanism in uranium binding is complex and includes both physisorption/chemisorption, ion exchange and surface complexation. The investigated biocomposite is a low cost and environmentally friendly sorbent with high potential for efficient U(VI) removal and recovery from aqueous solution.

Declarations

Conflict of interest The authors declare that they have no conflict of interest.

References

1. Gadd GM (2001) Phytoremediation of toxic metals; using plants to clean up the environment. J Chem Technol Biotechnol 76(3):325–325
2. Anirudhan TS, Divya L, Suchithra PS (2009) Removal and recovery of uranium (VI) by adsorption onto a lignocellulosic-based polymeric adsorbent containing amidoxime chelating functional group. Toxicol Environ Chem 91(7):1237–1252
3. Bayramoğlu G, Çelik G, Arica MY (2006) Studies on accumulation of uranium by fungus *Lentinus sajor-caju*. J Hazard Mater. https://doi.org/10.1016/j.jhazmat.2005.12.027
4. Fomina M, Gadd GM (2014) Biosorption: current perspectives on concept, definition, and application. Bioresour Technol 160:3–14
5. Khambhaty Y, Mody K, Basha S, Jha B (2009) Kinetics, equilibrium and thermodynamic studies on biosorption of hexavalent chromium by dead fungal biomass of marine *Aspergillus niger*. Chem Eng J 145:489–495
6. Genç Ö, Yalçınkay Y, Büyüktuncel E, Denizli A, Arıca MY, Bektaş S (2003) Uranium recovery by immobilized and dried powdered biomass: characterization and comparison. Int J Miner Process 68:93–107
7. Li X, Ding C, Liao J, Du L, Sun Q, Yang J, Yang Y, Zhang D, Tang J, Liu N (2016) Bioaccumulation characterization of uranium by a novel *Streptomyces sporoverrucosus* dwc-3. J Environ Sci 41:162–171
8. Bağda E, Tuzen M, Sarı A (2017) Equilibrium, thermodynamic and kinetic investigations for biosorption of uranium with green algae (*Cladophora hutchinsiae*). J Environ Radioact 175–176:7–14
9. Wang X, Yu S, Jin J, Wang H, Alharbi NS, Alsaedi A, Tasawar H, Wang X (2016) Application of graphene oxides and graphene oxide-based nanomaterials in radionuclide removal from aqueous solutions. Sci Bull 61(20):1583–1593
10. Chen Z, Zhang S, Liu Y, Alharbi NS, Rabah SO, Wang S. Wang X (2020) Synthesis and fabrication of g-C_3N_4-based materials and their application in elimination of pollutants. Sci Total Environ 139054
11. Wang X, Li X, Wang J, Zhu H (2020) Recent advances in carbon nitride-based nanomaterials for the removal of heavy metal ions from aqueous solution. J Inorg Mater 35(3):260–270
12. Chen L, Yang W, He X, Wang E, Xian Q, Dan H, Zhu W, Ding Y (2020) A convenient one-step synthesis of mesoporous ZrO_2/SBA-15 and its uranium adsorption properties. J Radioanal Nucl Chem 326(2):1027–1037
13. Dan H, Chen L, Xian Q, Yi F, Ding Y (2019) Tailored synthesis of SBA-15 rods using different types of acids and its application in adsorption of uranium. Sep Purif Technol 210:491–496
14. Ding Y, Xian Q, Wang E, He X, Jiang Z, Dan H, Zhu W (2020) Mesoporous MnO_2/SBA-15 as a synergetic adsorbent for enhanced uranium adsorption. New J Chem 44(32):13707–13715
15. Li Q, Liu Y, Cao X, Pang C, Wang Y, Zhang Z, Liu Y, Hua M (2012) Biosorption characteristics of uranium(VI) from aqueous solution by pummelo peel. J Radioanal Nucl Chem 293:67–73

16. Kausar A, Bhatti HN, MacKinnon G (2013) Equilibrium, kinetic and thermodynamic studies on the removal of U (VI) by low cost agricultural waste. Colloids Surf B Biointerfaces 111:124–133
17. Nuhanović M, Grebo M, Draganović S, Memić M, Smječanin N (2019) Uranium (VI) biosorption by sugar beet pulp: equilibrium, kinetic and thermodynamic studies. J Radioanal Nucl Chem 322:2065–2078
18. Šabanović E, Muhić-Šarac T, Nuhanović M, Memić M (2019) Biosorption of Uranium (VI) from aqueous solution by *Citrus limon* peels: kinetics, equlibrium and batch studies. J Radioanal Nucl Chem 319:425–435
19. Bagherifam S, Lakzian A, Ahmadi S, Rahimi M, Halajnia A (2010) Uranium removal from aqueous solutions by wood powder and wheat straw. J Radioanal Nucl Chem 283(2):289–296
20. Donat R, Aytas S (2005) Adsorption and thermodynamic behavior of uranium (VI) on *Ulva* sp.-Na bentonite composite adsorbent. J Radioanal Nucl Chem 265:107–114
21. Aytas S, Turkozu DA, Gok C (2011) Biosorption of uranium (VI) by bi-functionalized low cost biocomposite adsorbent. Desalination 280:354–362
22. Khan MH, Warwick P, Evans N (2006) Spectrophotometric determination of uranium with arsenazo-III in perchloric acid. Chemosphere 63:1165–1169
23. Akar T, Kaynak Z, Ulusoy S, Yuvaci D, Ozsari G, Akar ST (2009) Enhanced biosorption of nickel (II) ions by silica-gel-immobilized waste biomass: biosorption characteristics in batch and dynamic flow mode. J Hazard Mater 163:1134–1141
24. Zou W, Zhao L (2012) Removal of uranium(VI) from aqueous solution using citric acid modified pine sawdust: batch and column studies. J Radioanal Nucl Chem 292:585–595
25. Bayramoglu G, Arica MY (2016) Amidoxime functionalized *Trametes trogii* pellets for removal of uranium(VI) from aqueous medium. J Radioanal Nucl Chem 307:373–384
26. Bhatti HN, Hamid S (2014) Removal of uranium (VI) from aqueous solutions using *Eucalyptus citriodora* distillation sludge. Int J Environ Sci Technol 11:813–822
27. Oliveira RC, Hammer P, Guibal E, Taulemesse JM, Garcia O Jr (2014) Characterization of metal–biomass interactions in the lanthanum(III) biosorption on *Sargassum* sp. using SEM/EDX, FTIR, and XPS: preliminary studies. Chem Eng J 239:381–391
28. Zhang Y, Zhao J, Jiang Z, Shan D, Lu Y (2014) Biosorption of Fe(II) and Mn(II) ions from aqueous solution by rice husk ash. Biomed Res Int. https://doi.org/10.1155/2014/973095
29. Ferreira RVP, de Araujo LG, Canevesi RLS, da Silva EA, Ferreira EGA, Palmieri MC, Marumo JT (2020) The use of rice and coffee husks for biosorption of U (total), ^{241}Am, and ^{137}Cs in radioactive liquid organic waste. Environ Sci Pollut Res 27:36651–36663
30. Azouaou N, Sadaoui Z, Djaafri A, Mokaddem H (2010) Adsorption of cadmium from aqueous solution onto untreated coffee grounds: equilibrium, kinetics and thermodynamics. J Hazard Mater 184:126–134
31. Memon JR, Memon SQ, Bhanger MI, Memon GZ, El-Turki A, Allen GC (2008) Characterization of banana peel by scanning electron microscopy and FT-IR spectroscopy and its use for cadmium removal. Colloids Surf B Biointerfaces 66:260–265
32. Memon JR, Memon SQ, Bhanger MI, El-Turki A, Hallam KR, Allen GC (2009) Banana peel: A green and economical sorbent for the selective removal of Cr(VI) from industrial wastewater. Colloids Surf B Biointerfaces 70:232–237
33. Pathak PD, Mandavgane SA, Kulkarni BD (2016) Utilization of banana peel for the removal of benzoic and salicylic acid from aqueous solutions and its potential reuse. Desalin Water Treat 57:12717–12729
34. Iqbal M, Saeed A, Kalim I (2009) Characterization of adsorptive capacity and investigation of mechanism of Cu^{2+}, Ni^{2+} and Zn^{2+} adsorption on mango peel waste from constituted metal solution and genuine electroplating effluent. Sep Sci Technol 44:3770–3791
35. Iqbal M, Saeed A, Zafar SI (2009) FTIR spectrophotometry, kinetics and adsorption isotherms modeling, ion exchange, and EDX analysis for understanding the mechanism of Cd^{2+} and Pb^{2+} removal by mango peel waste. J Hazard Mater 164:161–171
36. Zhao X, Chen Y (2020) Adsorption of methylene blue using $FeCl_3$-modified pomelo peel. Russ J Phys Chem 94:835–845
37. Dinh VP, Huynh TDT, Le HM, Nguyen VD, Dao VA, Hung NQ, Tuyen LA, Lee S, Yi J, Nguyen TD, Van LV (2019) Insight into the adsorption mechanisms of methylene blue and chromium(III) from aqueous solution onto pomelo fruit peel. RSC Adv 9:25847–25860
38. Dinh VP, Xuan TD, Hung NQ, Luu TT, Do TTT, Nguyen TD, Nguyen VD, Anh TTK, Tran NQ (2020) Primary biosorption mechanism of lead (II) and cadmium (II) cations from aqueous solution by pomelo (*Citrus maxima*) fruit peels. Environ Sci Pollut Res. https://doi.org/10.1007/s11356-020-10176-6
39. Yi ZJ, Yao J, Zhu MJ, Chen HL, Wang F, Liu X (2017) Biosorption characteristics of *Ceratophyllum demersum* biomass for removal of uranium(VI) from an aqueous solution. J Radioanal Nucl Chem 313:19–27
40. Yi ZJ, Yao J (2012) Kinetic and equilibrium study of uranium (VI) adsorption by *Bacillus licheniformis*. J Radioanal Nucl Chem 293:907–914
41. Sun Y, Ding C, Cheng W, Wang X (2014) Simultaneous adsorption and reduction of U(VI) on reduced graphene oxide-supported nanoscale zerovalent iron. J Hazard Mater 280:399–408
42. Anirudhan TS, Bringle CD, Rijith S (2009) Removal of uranium(VI) from aqueous solution and nuclear industry effluents using humic acid-immobilized zirconium-pillared clay. J Environ Radioact 101:267–276
43. Boota R, Bhatti HN, Hanif MA (2009) Removal of Cu(II) and Zn(II) using lignocellulosic fiber derive from *Citrus reticulata* (Kinnow) waste biomass. Sep Sci Technol 44:4000–4022
44. Wang F, Tan L, Liu Q, Li R, Li Z, Zhang H, Hu S, Liu L, Wang J (2015) Biosorption characteristics of Uranium (VI) from aqueous solution by pollen pini. J Environ Radioact 150:93–98
45. Lagergren SY (1898) Zur Theorie der Sogenannten Adsorption Gelöster Stoffe, Kungliga Svenska Vetenskapsakademiens. Handlingar 24:1–39
46. Ho YS, McKay G (1999) Pseudo-second-order model for sorption processes. Process Biochem 34:451–465
47. Weber W Jr, Morris JC (1963) Kinetics of adsorption on carbon from solutions. J Sanit Eng Div 89:31–60
48. OuYang XK, Jin RN, Yang LP, Wen ZS, Yang LY, Wang YG, Wang CY (2014) Partially hydroliyzed Bamboo (*Phyllostachys heterocycla*) as a porous bioadsorbent for the removal of Pb(II) from aqueous mixtures. J Agric Food Chem 62:6007–6015
49. Langmuir I (1918) The adsorption of gases on plane surfaces of glass, mica and platinum. J Am Chem Soc 40:1361–1403
50. Freundlich HMF (1906) Over the adsorption in solution. J Phys Chem 57:385–471
51. Tempkin MI, Pyzhev V (1940) Kinetics of ammonia synthesis on promoted iron catalyst. Acta Phys Chim USSR 12:327–356
52. Babaeivelni K, Khodadoust AP (2013) Adsorption of fluoride onto crystalline titanium dioxide: effect of pH, ionic strength, and coexisting ions. J Colloids Interface Sci 394:419–427
53. Yuan Y, Liu N, Dai Y, Wang B, Liu Y, Chen C, Huang D (2020) Effective biosorption of uranium from aqueous solution by cyanobacterium *Anabaena flos-aquae*. Environ Sci Pollut Res. https://doi.org/10.1007/s11356-020-10364-4
54. Ai L, Luo X, Lin X, Zhang S (2013) Biosorption behaviors of uranium (VI) from aqueous solution by sunflower straw and insights of binding mechanism. J Radioanal Nucl Chem 298:1823–1834

55. Meena AK, Mishra GK, Rai PK, Rajagopal C, Nagar PN (2005) Removal of heavy metal ions from aqueous solutions using carbon aerogel as an adsorbent. J Hazard Mater 122:161–170
56. Gupta NK, Sengupta A, Gupta A, Sonawane JR, Sahoo H (2018) Biosorption-an alternative method for nuclear waste management: a critical review. J Environ Chem Eng. https://doi.org/10.1016/j.jece.2018.03.021
57. Bai J, Yin X, Zhu Y, Fan F, Wu X, Tian W, Tan C, Zhang X, Wang Y, Cao S, Fan F, Qin Z, Guo J (2016) Selective uranium sorption from salt lake brines by amidoximated *Saccharomyces cerevisiae*. Chem Eng J 283:889–895
58. Akhtar K, Akhtar MW, Khalid AM (2007) Removal and recovery of uranium from aqueous solutions by *Trichoderma harzianum*. Water Res 41:1366–1378
59. Noli F, Kapashi E, Kapnisti M (2019) Biosorption of uranium and cadmium using sorbents based on Aloe vera wastes. Journal of Environmental Chemical Engineering 7(2):102985
60. Hadavifar M, Bahramifar N, Younesi H, Li Q (2014) Adsorption of mercury ions from synthetic and real wastewater aqueous solution by functionalized multi-walled carbon nanotube with both amino and thiolated group. Chem Eng J 237:217–228
61. Sahmoune MN (2019) Evaluation of thermodynamic parameters for adsorption of heavy metals by green adsorbents. Environ Chem Letters 17(2):697–704
62. El-Araby HA, Ibrahim AMMA, Mangood AH, Adel AH (2017) Sesame husk as adsorbent for copper (II) ions removal from aqueous solution. J Geosci Environ Protect 5(07):109
63. Hema M, Arivoli S (2008) Adsorption Kinetics and Thermodynamics of Malachite Green Dye unto Acid Activated Low Cost Carbon. J Appl Sci Environ Manage 12:43–51
64. Denizli A, Say R, Arica Y (2000) Removal of Heavy Metal Ions from Aquatic Solutions by Membrane Chromatography. Separat Purifi Technol 21:181–190
65. Li Q, Liu Y, Cao X, Pang C, Wang Y, Zhang Z, Liu Y, Hua M (2012) Biosorption characteristics of uranium (VI) from aqueous solution by pummelo peel. J Radioanal Nucl Chem 293(1):67–73
66. Donat R, Cılgı G, Aytas S, Cetisli H (2009) Thermodynamic parameters and sorption of U (VI) on ACSD. J Radioanal Nucl Chem 279(1):271–280
67. Yang T, Zhang W, Liu H, Guo Y (2020) Enhanced removal of U (VI) from aqueous solution by chitosan-modified zeolite. J Radioanal Nucl Chem 323(2):1003–1012